



## Exotic Dense-Matter States Pumped by a Relativistic Laser Plasma in the Radiation-Dominated Regime

J. Colgan,<sup>1</sup> J. Abdallah, Jr.,<sup>1</sup> A. Ya. Faenov,<sup>2,9</sup> S. A. Pikuz,<sup>2</sup> E. Wagensars,<sup>3</sup> N. Booth,<sup>4</sup> O. Culfa,<sup>3</sup> R. J. Dance,<sup>3</sup> R. G. Evans,<sup>5</sup> R. J. Gray,<sup>6</sup> T. Kaempfer,<sup>7</sup> K. L. Lancaster,<sup>4</sup> P. McKenna,<sup>6</sup> A. L. Rossall,<sup>3</sup> I. Yu. Skobelev,<sup>2</sup> K. S. Schulze,<sup>7</sup> I. Uschmann,<sup>7,10</sup> A. G. Zhidkov,<sup>8</sup> and N. C. Woolsey<sup>3</sup>

<sup>1</sup>Theoretical Division, Los Alamos National Laboratory, Los Alamos, New Mexico 87545, USA

<sup>2</sup>Joint Institute for High Temperatures, Russian Academy of Sciences, Moscow 125412, Russia

<sup>3</sup>York Plasma Institute, Department of Physics, University of York, York YO10 5DD, United Kingdom

<sup>4</sup>Central Laser Facility, STFC Rutherford Appleton Laboratory, Didcot, Oxfordshire OX11 0QX, United Kingdom

<sup>5</sup>Department of Physics, Imperial College, London SW7 2AZ, United Kingdom

<sup>6</sup>SUPA, Department of Physics, University of Strathclyde, Glasgow G4 0NG, United Kingdom

<sup>7</sup>Helmholtzinstitut Jena, Fröbelstieg 1, D-07743 Jena, Germany

<sup>8</sup>PPC Osaka University and JST, CREST, 2-1, Yamadaoka, Suita, Osaka 565-0871, Japan

<sup>9</sup>Quantum Beam Science Directorate, Japan Atomic Energy Agency, Kizugawa, Kyoto 619-0215, Japan

<sup>10</sup>Institut für Optik und Quantenelektronik, Friedrich-Schiller-Universität Jena, Max-Wien Platz 1, D-07743 Jena, Germany

(Received 31 October 2012; published 18 March 2013)

In high-spectral resolution experiments with the petawatt Vulcan laser, strong x-ray radiation of *KK* hollow atoms (atoms without  $n = 1$  electrons) from thin Al foils was observed at pulse intensities of  $3 \times 10^{20}$  W/cm<sup>2</sup>. The observations of spectra from these exotic states of matter are supported by detailed kinetics calculations, and are consistent with a picture in which an intense polychromatic x-ray field, formed from Thomson scattering and bremsstrahlung in the electrostatic fields at the target surface, drives the *KK* hollow atom production. We estimate that this x-ray field has an intensity of  $>5 \times 10^{18}$  W/cm<sup>2</sup> and is in the 3 keV range.

DOI: [10.1103/PhysRevLett.110.125001](https://doi.org/10.1103/PhysRevLett.110.125001)

PACS numbers: 52.20.Hv, 34.80.Dp, 52.25.Jm

The properties of high energy density plasma have been under increasing scrutiny in recent years due to their importance to our understanding of stellar interiors, the cores of giant planets [1], and hot plasma in inertial confinement fusion devices [2]. Such studies are also relevant to photoionized plasmas found in active galactic nuclei and x-ray binaries [3]. Currently, powerful x-ray free-electron-laser sources (XFELs) are being used to create such high energy density matter [4,5] using x rays at intensities greater than  $10^{17}$  W/cm<sup>2</sup>. The radiation intensity dominates standard collisional atomic processes creating exotic states of matter, composed of hollow atoms, which are diagnosed through the observation of unique spectral lines [6]. Although the definition of a hollow atom is not unique [7–9], it is usually taken to mean atoms (or ions) in which *K* and/or *L* shell electrons have been removed in preference to the valence electrons.

In this work, we report the observation of hollow atoms with double *K*-shell (principal quantum number  $n = 1$ ) vacancies (*KK* atoms) formed with long-wavelength laser fields. This might be regarded as unexpected since the small photon energies of the laser pulse cannot directly ionize the target *K*-shell electrons. Our detailed atomic kinetics simulations suggest that an intense short-wavelength radiation field is the only plausible mechanism for production of hollow atoms. We provide a detailed argument for the generation of this intense x-ray radiation

field through the energy loss of the highly accelerated field-ionized electrons produced from the intense long-wavelength laser field. This work complements the recent observations of such exotic states using XFELs [4,5]. We note that the radiation field generated in our experiments is polychromatic with an intensity that is comparable to or exceeding that of current XFELs. Our work implies that matter dominated by exotic hollow atom states, as well as radiation-dominated atomic physics, can be accessed and probed with high-power optical lasers. Indeed, as laser intensities continue to increase above  $10^{22}$  W/cm<sup>2</sup>, radiation processes will start to govern plasma interaction physics as well as the atomic physics [10–12]. The proposed concept and experimental layout is schematically shown in Fig. 1.

The measurements were made at the Vulcan Petawatt (PW) Laser Facility at Rutherford Appleton Laboratory, which provides a beam using optical parametric chirped pulse amplification technology with a central wavelength of 1054 nm and a pulse FWHM duration of 0.7 ps. The optical parametric chirped pulse amplification approach enables an amplified spontaneous emission to peak-intensity contrast ratio exceeding  $1:10^9$  several nanoseconds before the peak of the laser pulse. The laser pulse was focused with an  $f/3$  off-axis parabola providing up to 160 J on the target. The maximum laser intensity of  $3 \times 10^{20}$  W/cm<sup>2</sup> was achieved with a laser focus

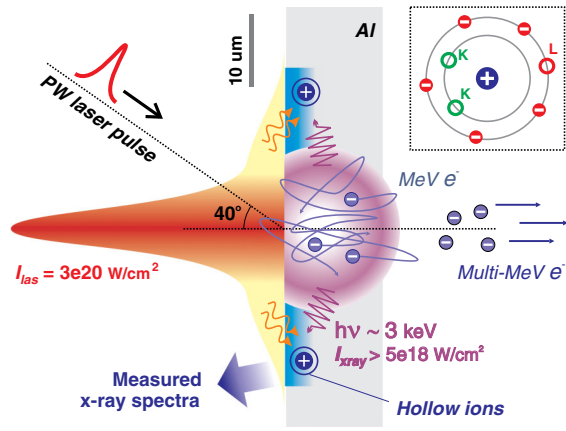


FIG. 1 (color online). A schematic diagram of hollow atom formation by the ultraintense optical laser pulse. A laser field of  $10^{20}$  W/cm<sup>2</sup> in the central area of the focal spot accelerates MeV and multi-MeV electrons from a target and produces bright x-ray radiation range via Thomson scattering and bremsstrahlung processes. In turn, the x-ray photons of  $\sim$ keV energies, produced in an almost perpendicular direction with respect to the laser beam propagation, create hollow atoms in the outer area of the focal spot.

containing approximately 30% of the energy in an  $8 \mu\text{m}$  (FWHM) diameter spot. The  $p$ -polarized laser beam was incident on target at  $40^\circ$  from the target surface normal.

Aluminum  $K$ -shell emission spectra from samples of various thicknesses were measured using a focusing spectrometer with spatial resolution equipped with spherically bent mica crystals. The focusing spectrometer with spatial resolution was tuned to observe radiation in the wavelength range from  $7.0$  to  $8.4 \text{ \AA}$  containing the  $K$ -shell spectra from multicharged ions and neutral (i.e.,  $K_\alpha$ ) Al. The spectral resolving power is  $5000$ . The spectra were acquired from the front, laser irradiated surface, at  $45^\circ$  to the target normal. The corresponding spectra are shown in Fig. 2. The accepted wavelengths for the  $\text{Ly}_\alpha$ ,  $\text{He}_\alpha$ , and  $K_\alpha$  lines are indicated by the vertical dashed lines. The measured resonance line centers are shifted to longer wavelengths with respect to National Institute of Standard and Technology values by  $10$  and  $20$ – $25 \text{ m\AA}$ , respectively. We attribute this to a strong dense plasma effect and receding ion motion [13,14]. The black curve in the lower panel represents the data obtained from a  $1.5 \mu\text{m}$  thin Al foil irradiated with  $160 \text{ J}$  on target, the maximum available.

As shown in the lower panel of Fig. 2, the reduction of the laser pulse energy from  $160$  to  $64 \text{ J}$  as the intensity drops  $40\%$  to around  $10^{20}$  W/cm<sup>2</sup> leads to remarkable changes in the spectra. For the lower laser energy case ( $64 \text{ J}$ ), we observe little emission, with prominent peaks just below  $7.8$  and  $7.2 \text{ \AA}$  corresponding to  $\text{He}_\alpha$  and  $\text{Ly}_\alpha$  transitions. Some satellites to these lines can also be observed. In the full laser energy case ( $160 \text{ J}$ ) the  $\text{He}_\alpha$  and  $\text{Ly}_\alpha$  lines are dominated by significant and striking emission between  $7.3$  and  $7.7 \text{ \AA}$  (which we

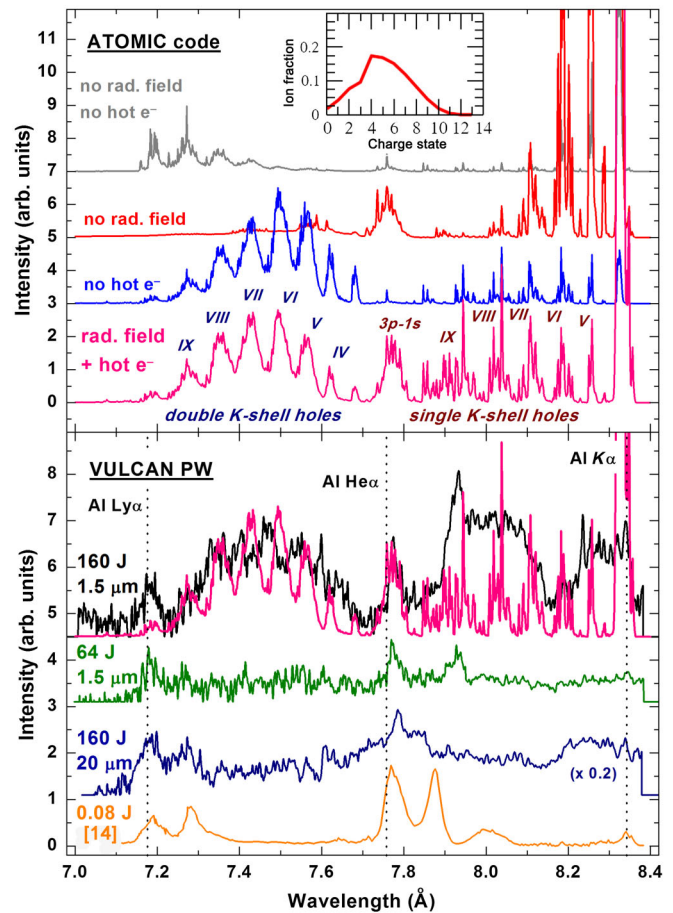


FIG. 2 (color online). Aluminum  $K$ -shell spectra calculated by the ATOMIC code (upper panel) and measured at the Vulcan PW laser (lower panel). ATOMIC calculations are made at plasma conditions as indicated in the text and for different options as indicated. The inset shows the ion charge distribution for the combined calculation (pink line in both panels) that includes the radiation field and hot electrons. Experimental spectra were measured for Al foil targets of  $1.5$  or  $20 \mu\text{m}$  thickness and with laser energies of  $160$  or  $64 \text{ J}$ . As a reference the lowest curve represents the data obtained at  $5 \times 10^{17}$  W/cm<sup>2</sup> intensity [15]. The vertical dashed lines indicate the Al  $\text{Ly}_\alpha$ ,  $\text{He}_\alpha$ , and  $K_\alpha$  transitions. All plots are offset vertically, and the data for the  $20 \mu\text{m}$  Al target are multiplied by a factor of  $0.2$ , for better visibility and convenient comparison.

identify below as arising from  $KK$  hollow atoms) and between  $7.9$  and  $8.3 \text{ \AA}$  (which below we associate with emission from  $KL$  hollow atoms). These spectra differ notably from observations previously made with optical lasers. For reference, more “usual” spectra [15] obtained using a much lower laser intensity of  $5 \times 10^{17}$  W/cm<sup>2</sup> are also presented in Fig. 2 (lowest curve).

Our atomic physics analysis, discussed below, shows that emission arises primarily from transitions between the  $n = 1$  and  $n = 2$  energy levels from Al hollow atoms from ionization stages Al III through Al X. The spectrum between  $7.3$  and  $7.7 \text{ \AA}$  is due to emission from ions with

two electrons missing from the  $n = 1$  level (labeled  $KK$  states) and the spectrum between 7.9 and 8.3 Å is due to emission from a state ( $KL$ ) with a single vacancy in both the  $n = 1$  and  $n = 2$  levels. The analysis implies that for such emission to be observed the emitting region must be immersed in a x-ray radiation field of keV energies and of extreme intensity, and additionally implies that the electron density is high, greater than  $10^{23}$  cm $^{-3}$ . At these conditions, the three-body recombination drives the ions back towards the neutral stage.

The lower panel of Fig. 2 also presents the spectrum measured from 20 μm thick targets irradiated at the highest laser intensity (160 J). These spectra show a marked drop in hollow atom emission. This appears to be a consequence of a less intense x-ray radiation field.

A keV radiation field interacts with the inner atomic shells of the Al ions and will eject multiple  $K$ - and  $L$ -shell electrons. Inner-shell electrons are preferentially ionized (compared to valence electrons) by high-energy photons so that the excess recoil momentum can be absorbed by the nucleus. Photons with energies close to the  $K$ -shell ionization potential at 1.5 keV (for Al) or higher are much more efficient at removing  $K$ -shell electrons than electrons of similar energies [8]. Consideration of the photoionization cross sections and autoionization decay rates leads to an estimate of the x-ray flux of at least  $10^{18}$  W/cm $^2$  required to produce  $KK$  hollow ions. A previous measurement [16], which used similar laser intensities to the present measurement but a much thicker target and lower contrast, found that electron pumping of  $KL$  hollow ions was the main ionizing mechanism and that the generation of  $KK$  hollow ions was not efficient.

X-ray spectra were studied by performing atomic kinetics calculations using the ATOMIC code [17]. Time-dependent calculations using a simplified atomic model were performed to determine the bulk plasma conditions. These calculations show that, at the high electron densities under consideration here, the system reaches steady state very quickly, within 1 ps. We then performed detailed steady-state calculations at various plasma conditions to compute the emission spectrum as a function of electron temperature (including non-Maxwellian effects such as hot electron tails) and density and radiation temperature. We assumed that the radiation field seen by the plasma was a Planckian distribution in the keV range. Our calculations include all relevant atomic processes, that is, photoionization, collisional ionization, autoionization, collisional and radiative excitation and deexcitation, and all recombination processes.

The collisional-radiative rate equations are solved to produce a set of ion populations that depends sensitively on the electron temperature and density, the radiation field, and the fraction of energetic electrons included in our model. Opacity effects are included via escape factors. The resulting level populations are used to produce

emission spectra, where the effects of detailed lines are included via a mixed unresolved transition array approach [18]. To correctly model the exotic plasma created experimentally, it is necessary to include over 16 000 configurations, representing Al ions in which up to five electrons have been removed from the  $K$  and  $L$  shells and placed in excited states. Multiply excited states were found to be important in accurately reproducing the observed emission spectrum. In particular, we find that the radiative decay from the  $L$  to  $K$  shell in any one specific configuration results in a relatively weak line, but that the very large number of configurations with different combinations of spectator electrons in excited states, in which this radiative transition occurs, allows the observed transition to become prominent.

The upper panel of Fig. 2 shows ATOMIC calculations modeled by a plasma exposed to a radiation field ( $T_r$ ) peaked at 3 keV, with a bulk electron temperature ( $T_e$ ) of 55 eV and electron density ( $N_e$ ) of  $3 \times 10^{23}$  cm $^{-3}$ , with ion number density of  $5.9 \times 10^{22}$  cm $^{-3}$ . A small fraction (5%) of the electron distribution was in a hot-electron tail with a temperature of 5 keV. A  $T_e$  of 55 eV was chosen as this value gave the best fit to the hollow ion spectra. Inclusion of a hot-electron tail includes the effects of electrons that have not fully thermalized. The collisional-radiative picture is highly nonequilibrium, in that the ionization is driven by photoionization from the radiation field, and recombination is driven mostly through three-body recombination due to the high electron density.

The full calculation is the lower pink line in the upper panel of Fig. 2, and we find clear evidence of emission from hollow ions from a range of Al charge states as labeled. The pink spectrum is a composite of the full ATOMIC calculation and several calculations at more moderate conditions ( $N_e = 10^{22}$  cm $^{-3}$ ,  $T_r = 50$  eV,  $T_e = 10, 20,$  and  $40$  eV) that were made to model the wavelength region between 7.8 and 8.3 Å. The comparison with the measured spectrum (black and pink lines at the top of the lower panel of Fig. 2) shows that the composite atomic kinetics calculation successfully reproduces most of the significant and striking features of the measurement. We find that transitions involving double  $K$ -shell holes (between 7.2 and 7.7 Å) are visible for a range of Al ions from Al IV through Al IX. Emission lines have been identified that arise from ions with up to five inner electrons removed from the  $K$  and  $L$  shell. We also observe significant emission at higher wavelengths (7.7 and 8.3 Å) from single  $K$ -shell holes, again from a range of Al ions as indicated. The calculations support a picture in which this emission is from plasma at lower densities interacting with x-ray radiation field of much reduced intensity.

To demonstrate that the intense x-ray radiation field is responsible for the calculated double  $K$ -shell hollow ion emission, we also show two spectra (gray and red lines) in the upper panel of Fig. 2, with no radiation field included in

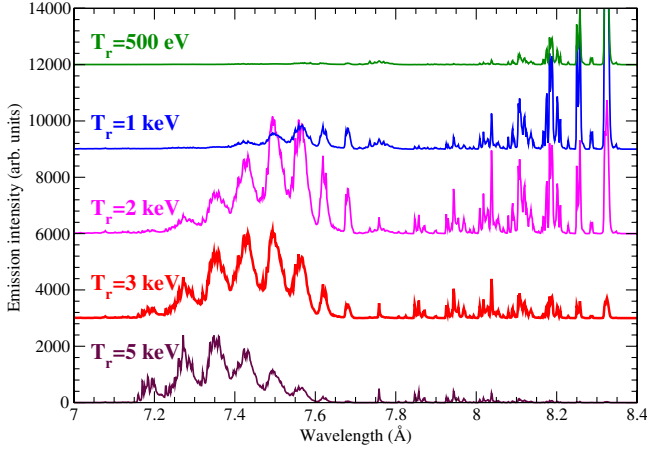


FIG. 3 (color online). Al  $K$ -shell spectra calculated by the ATOMIC code at plasma conditions discussed in the text and at the radiation temperatures ( $T_r$ ) indicated. The spectra are offset for better visibility.

the calculation. Virtually no emission lines due to hollow ions are observed. The red line shows the influence of the 5 keV hot-electron tail on the emission spectrum. It is clear that the radiation field has a dramatic effect. In Fig. 2 the blue line shows the effect of radiation on the calculation while omitting the hot-electron tail. We find that the hot electrons do excite  $KL$  hollow ions, but provide only a small part of the measured intensity of the  $KK$  hollow ion spectral lines.

In Fig. 3 we show ATOMIC calculations for the same conditions as in Fig. 2 and with a systematic variation in  $T_r$ . We find that at a  $T_r$  of 500 eV there are no lines emitted in the 7.2–7.7 Å region, which is not surprising since this radiation temperature is below the  $K$ -shell ionization potential. However, for  $T_r = 2$  keV, we see a dramatic change; a series of intense lines is now prominent. As we move to  $T_r = 3$  keV the intensity of these features is modified somewhat (and is in better agreement with the observed spectrum). As  $T_r$  is increased to 5 keV, the intensity of the spectral features between 7.2 and 7.7 Å is in poorer agreement with the measured spectrum. Although we have modeled the radiation field as a Planckian distribution, it is possible that the radiation field that produces the measured spectra is not fully thermalized. Our collisional-radiative simulations using a 3 keV Planckian radiation field does, however, reproduce the essential features of this time-integrated measurement. We regard the influence of an intense radiation field as the only plausible mechanism for generation of  $KK$  hollow atoms.

To understand how a x-ray radiation field at keV energies could be generated in these experiments, we recall that the Vulcan PW laser rapidly ionizes valence electrons from the Al target through field ionization [19] and ponderomotively accelerates electrons to energies of a few MeV [20]. During the interaction of an intense laser pulse with a thin foil some of these highly energetic electrons oscillate

between the front and rear surfaces of the foil [19,21], due to reflection by the electrostatic and magnetic fields on each surface, known as refluxing. The thin Al target is essentially transparent to these highly relativistic electrons [19], but the electrons quickly lose energy through bremsstrahlung [22] in the surface plasma fields and (nonlinear) Thomson scattering [23,24]. The scaling of the radiation power  $P$ , with the laser amplitude  $a_0 = eE/mc\omega$  (where  $E$  is the electric field strength,  $\omega$  the field frequency,  $m$  the electron mass, and  $c$  the speed of light), can be estimated [10] with the use of the radiation friction force. According to Ref. [24] and after an integration, one can show that  $P \sim T_h^2 E^2 e^{-\epsilon(\theta)/T_h}$ , where  $T_h$  the temperature of the energetic electrons and  $\epsilon(\theta)$  is a minimal electron energy required to generate x rays into an angle between  $\theta$  and  $\theta + \Delta\theta$ . Here,  $\theta$  is the angle between the direction of the emitter motion and the direction to the observer—i.e., the angle between the normal to the target surface (as the predominant direction of electron flow) and the hollow atom location. The strength of the field in all radiation processes is proportional to  $a_0$ , whereas the temperature has a more complicated dependency; it is proportional to  $a_0$  in an overdense plasma and to  $a_0^2$  in an underdense plasma. Hence, we can say  $P \sim [a_0^4 - a_0^6]e^{-\epsilon(\theta)/T_h}$ . If  $\epsilon(\theta)$  far exceeds  $T_h$ , then the power rapidly increases with  $a_0$  and quickly becomes zero at lower intensities.

This strong dependence explains why the reduction of the laser pulse energy from 160 to 64 J changes the observed emission spectra in Fig. 2 so dramatically. For laser intensities of  $3 \times 10^{20}$  W/cm<sup>2</sup>, we find that the resulting x-ray intensity exceeds  $5 \times 10^{18}$  W/cm<sup>2</sup> [24]. For  $\theta$  values of several degrees, the radiated photon energy from a few MeV electron beam is  $\sim 3$  keV. This analysis also explains why the spectrum measured from the 20  $\mu$ m thick target showed much weaker hollow atom emission. Refluxing in a thicker target takes longer than in the thinner 1.5  $\mu$ m target. The fast electrons interact with the laser and plasma fields more frequently in the thinner target resulting in efficient radiation production via Thomson scattering and bremsstrahlung.

Within the center of the focal spot, the extreme laser intensity will strip virtually all the electrons from the Al atoms. For hollow atom formation, our analysis suggests that the Al ions must be subjected to a lower bulk temperature such as found at the periphery of the focal region. This is consistent with our radiation field model since we find that the 3 keV emission occurs at angles of a few degrees to the oscillating beam.

To conclude, the measurements, simulations, and physics picture discussed in this work are all consistent with a scenario in which high-intensity laser technology can be used to generate extremely intense polychromatic x-ray fields that enable experiments that complement those delivered by XFELs. In this case, we observe radiation-dominated atomic kinetics with matter ionized

predominantly through the inner-shell processes. The radiation field intensities are sufficiently extreme to generate copious double  $K$ -shell holes, true hollow atoms. This occurs at angles at which the radiation field photon energy is resonant with the  $K$  and  $KK$  ionization potentials. These exotic states appear to form in regions surrounding the laser focal spot. Finally, our results demonstrate how laser-plasma interaction physics will change as laser intensities move towards the radiation-dominant regime [11,12]. We plan further theoretical and experimental exploration of the very challenging and complex physics in such regimes.

We thank the Vulcan technical and target preparation teams at the Central Laser Facility for their support during the experiments. The research leading to these results has received funding from the Science and Technology Facilities Council and the Engineering and Physical Science Research Council (Grant No. EP/E048668/1) of the United Kingdom. The Los Alamos National Laboratory is operated by Los Alamos National Security, LLC for the NNSA of the U.S. DOE under Contract No. DE-AC5206NA25396. The work is supported by a mutual grant of the RFBR and Royal Society No. 12-02-92617-KOa and No. E120059 and RF President Grant No. MK-4725.2012.8.

- 
- [1] G. Chabrier, *Plasma Phys. Controlled Fusion* **51**, 124014 (2009).
- [2] S. Atzeni and J. Meyer-Ter-Vehn, *The Physics of Inertial Fusion* (Clarendon, Oxford, England, 2004).
- [3] E. Behar, M. Sako, and S. M. Kahn, *Astrophys. J.* **563**, 497 (2001).
- [4] S. M. Vinko *et al.*, *Nature (London)* **482**, 59 (2012).
- [5] L. Young *et al.*, *Nature (London)* **466**, 56 (2010).
- [6] B. Nagler *et al.*, *Nat. Phys.* **5**, 693 (2009).
- [7] J.-P. Briand, L. de Billy, P. Charles, S. Essabaa, P. Briand, R. Geller, J. P. Desclaux, S. Bliman, and C. Ristori, *Phys. Rev. Lett.* **65**, 159 (1990).
- [8] A. McPherson, B. D. Thompson, A. B. Borisov, K. Boyer, and C. K. Rhodes, *Nature (London)* **370**, 631 (1994).
- [9] I. Yu. Skobelev, A. Ya. Faenov, T. A. Pikuz, and V. E. Fortov, *Phys. Usp.* **55**, 47 (2012).
- [10] A. Zhidkov, J. Koga, A. Sasaki, and M. Uesaka, *Phys. Rev. Lett.* **88**, 185002 (2002).
- [11] C. P. Ridgers, C. S. Brady, R. Ducloux, J. G. Kirk, K. Bennett, T. D. Arber, A. P. L. Robinson, and A. R. Bell, *Phys. Rev. Lett.* **108**, 165006 (2012).
- [12] T. Nakamura, J. K. Koga, T. Zh. Esirkepov, M. Kando, G. Korn, and S. V. Bulanov, *Phys. Rev. Lett.* **108**, 195001 (2012).
- [13] A. Saemann, K. Eidmann, I. E. Golovkin, R. C. Mancini, E. Andersson, E. Förster, and K. Witte, *Phys. Rev. Lett.* **82**, 4843 (1999).
- [14] U. Andiel, K. Eidmann, P. Hakel, R. C. Mancini, G. C. Junkel-Vives, J. Abdallah, and K. Witte, *Europhys. Lett.* **60**, 861 (2002).
- [15] U. Andiel, K. Eidmann, K. Witte, I. Uschmann, and E. Forster, *Appl. Phys. Lett.* **80**, 198 (2002).
- [16] R. G. Evans *et al.*, *Appl. Phys. Lett.* **86**, 191505 (2005).
- [17] N. H. Magee *et al.*, in *Proceedings of the 14th Topical Conference on Atomic Processes in Plasmas*, edited by J. S. Cohen, S. Mazevet, and D. P. Kilcrease, AIP Conf. Proc. 730 (AIP, New York, 2004), pp. 168–179.
- [18] S. Mazevet and J. Abdallah, Jr., *J. Phys. B* **39**, 3419 (2006).
- [19] A. Zhidkov and A. Sasaki, *Phys. Plasmas* **7**, 1341 (2000).
- [20] M. Gavrilu, *Atoms in Intense Laser Fields* (Academic, New York, 1992).
- [21] P. Antici *et al.*, *Phys. Plasmas* **14**, 030701 (2007).
- [22] S. Nozawa, N. Itoh, and Y. Kohyama, *Astrophys. J.* **507**, 530 (1998).
- [23] E. S. Sarachik and G. T. Schappert, *Phys. Rev. D* **1**, 2738 (1970).
- [24] L. Landau and E. Lifshitz, *The Classical Theory of Fields* (Pergamon, London, 1961).